

Quantitative Structure Activity Relationship and Molecular Docking of Pim-1 Kinase Inhibitors

Rathod H*

Department of Biotechnology, University of Hyderabad, India

Abstract

QSAR has established itself as an important means of virtual screening. Computational analysis of numerous drug molecules aided the facility to meaningfully screen specific ones for further use and experimentation. In this study, three-dimensional quantitative structure-activity relationship (3D-QSAR) associated simulations were done and stochastic models were developed considering 55 molecules of hydroxyflavanone, thiazolidene2, 4-dione, pyridone derivatives against proviral insertion site of moloney murine leukemia virus. As part of the study, molecular field analysis (MFA) was done along with receptor surface analysis (RSA). Moreover, the generalization ability of the developed model was rigorously validated using 12 test set molecules. Molecular docking exercises were performed to analyze the protein structure using the crystal structure of PIM-1 kinase. Good correlation between predicted fitness scores and the observed activities was obtained. The presence of the hydroxyl groups in B ring instead of a ring was found crucial and playing important role for the compound activity. B ring substitution showed enhanced activity in this scenario. Further, the steric descriptor coefficient present near the ortho-position of N4 amine group indicates that any steric group increases the activity. GOLD was used for molecular docking of 55 molecules considered to target PIM-1 ATP binding site. GOLD based predicted fitness scores showed excellent correlation with the observations found in the available experimental outcomes.

Keywords: PIM-1 kinase; 3D-QSAR; GOLD molecular docking; Molecular field analysis; Receptor surface analysis; Molecular shape analysis; Receptor surface model

Introduction

Novel gene finding associated with tumorigenesis revealed that Pim-1 gene acts as a proviral insertion which was established experimentally in Moloney Murine Leukemia Virus (MoMuLV) [1]. In murine lymphoma associated succeeding experiments it was found that the same gene (Pim-1) loci some transcription factors (c-Myc and Gfi1) were regularly present in the retroviral insertion sites. Interestingly, similar factors were found to have an important role in T-cell associated lymphomagenesis.

Thus, concise investigative evidence was established in connecting the proto-oncogene Pim-1 and malignancy. Further scientific exploration revealed two more similar kinases which are known as Pim-2 and Pim-3. All these three kinase proteins are well conserved in vertebrates and show high degrees of sequence and structural similarities. Out of these 3 malignancy inducing genes, Pim-2 was found much active in rapid development of malignant T-cell lymphomas [2]. Reports suggest that the Pim-1 and Pim-3 is having identity of almost 72% and the 3rd type of Pim is present in mammalian cells. Compare to the other two types, oncology related studies on Pim-3 is not done much till now. In a specific experiment, recently it has been presented that Pim-3 gets up-regulated in Ewing's tumor cell lines. Alongside, it was found that the protein aids in elevation of anchorage independent cell growth in an in vivo tissue culture system. Pim-1 is highly expressed in thymus, fetal liver, spleen, and bone marrow. In parallel, expression of this protein is found in oral epithelia, hippocampus and cells of prostate which are non-hematopoietic type of tissues [1]. Furthermore, many tissue culture cells that stem from human tumors express Pim-1, examples are HeLa cells, the leukemia cell line K562 and a number of other myeloid and lymphoid tumor and prostate tumor lines. The Pim-1 protein is found both in the cytoplasm and in the nucleus. It was observed that Pim-1 protein is regulated by eIF 4E at post transcription stage and stabilized by Hsp90 and degraded by PP2A [3-7]. Pim-1 is

a downstream effector of many cytokine signaling pathways and the expression of the Pim-1 gene is induced by a large set of cytokines [1]. For instance, Pim-1 deficient cells show a disturbance in the IL-3/-7 dependent proliferation of mast cells and pre B-cells in bone marrow. Pim-1 expression is further induced by the STAT in relation to cytokine signaling. For instance, STAT3 is activated by many interleukins, IFN, c-Kit, SCF, G-CSF and EGF similar to STAT5, which is activated in particular by IL-2 and IL-7, Prolactin, G-CSF and GM-CSF [8-13]. Both STAT3/STAT5 can bind directly to the Pim-1 promoter at the ISFR/GAS-sequence (gamma interferon activation sequences). This molecular event accelerates the up regulation of Pim-1 (reference). In addition, Pim-1 itself can negatively regulate the Jak/STAT pathway by binding to a group of negative regulators of STAT activity, the so-called SOCS proteins. Little is known about the maintenance of Pim-1 protein levels and the stability of Pim-1 that may aid in the enhancement of Pim-1 protein expression level by the eukaryotic translation initiation factor 4 E (eIF-4E). Experimentally, antagonistic effect for reduction of Pim-1 protein expression is also hinted via the overexpression of serine/threonine phosphatase PP2A [14].

In addition, there is evidence that the Hsp90 protein is accountable for correct folding and stabilization of the Pim-1 protein [15-19]. The underlying mechanisms have not been investigated and remain to be discovered.

*Corresponding author: Rathod H, Department of Biotechnology, University of Hyderabad, Telangana 500046, India, Tel: +91 40-23134730; E-mail: rathod_h@rediffmail.com

Received October 31, 2016; Accepted December 26, 2016; Published January 10, 2017

Citation: Rathod H (2016) Quantitative Structure Activity Relationship and Molecular Docking of Pim-1 Kinase Inhibitors. Int J Biomed Data Min 6: 124. doi: 10.4172/2090-4924.1000124

Copyright: © 2016 Rathod H. This is an open-access article distributed under the terms of the Creative Commons Attribution License, which permits unrestricted use, distribution, and reproduction in any medium, provided the original author and source are credited.

In order to identify Pim-1 substrates, several binding partners of Pim-1 have been identified [1]. Many of them are linked with the cell cycle regulation followed by apoptosis. The first binding partner identified as a Pim-1 substrate was the nuclear adapter protein p100, which is an activator of the c-Myb transcription factor. NFATc, a transcription factor, was found to be involved in relaying signals from the T-cell receptor. Recently, interaction of Pim-1 and Bad, a pro-apoptotic protein, was discovered [20-22]. Direct evidence of involvement of Pim-1 in cell cycle progression was documented from the experimentally proved binding of Pim-1 and phosphatase Cdc25A, a positive G1-specific cell cycle regulator. Moreover, most recently, the proteins C-TAK1 and Cdc25C were also identified as Pim-1 substrates (reference). Both proteins play important roles in cells that are in transition from the G2 phase into mitosis [1].

More scientific investigations suggested that the Pim-1 protein is responsible for interacting in many signaling pathways in relation to the molecular control processes of hematopoiesis and lymphopoiesis. Furthermore, Pim-1 is over expressed or even mutated in a number of tumors and in different types of tumor cell lines which leads to genomic instability of the particular cell. Examples for a possible involvement of Pim-1 in human tumors are prostate cancer, oral cancer or Burkitt lymphoma, all these findings point to an important role of Pim-1 in the initiation or progression of human cancer. However, considering Pim-1 as a target for therapeutic purpose is an independent fact and will not be related to the obtained results of typical target validation experiments but also on the suitability of Pim-1 to be modified by drugs and other catalysts.

The expression of Pim-1 is directly regulated through both latent transcription factors STAT3 and STAT5. Activation of STAT is done by the JAKs which is further dependent on the excitation of cytokine receptor via other factors such as growth factor or interleukins. STAT3 is negatively regulated through Pias3 and p53. Pias3 itself is inhibited by the onco-protein Gfi1. Pim-1 is used as a catalyst for phosphorylation of other proteins in a pathway and causes activation and inactivation of number of important proteins, thus, having a role in apoptosis and other cellular events concerning cell cycle regulation [1].

The human, murine or rat PIM-1 proteins, all contain 313 amino acids with a sequence similarity of 94% (human/ mouse) or 97% (human/rat). An interesting fact was found for the *Xenopus laevis* Pim-1 protein. The protein is having 323 amino acids but so far, no function associated information is available for the additional 10 amino acids [1,23]. The Pim-1 gene encodes two proteins of 34 and 44 kD due to the use of an event of alternative translation.

Pim-1 kinase catalytic region ranges from 38–290 residue position in the protein, a specific highly conserved motif related to the glycine loop is present at 45-50 residue position. A phosphate binding site at residue positions 44–52 and 67 and a proton acceptor site at residue 167. The replacement of a lysine at position 67 by a methionine results in a kinase inactive Pim-1 mutant.

The Pim-1 complex structure shows a unique feature that distinguishes Pim-1 from all other kinases in the hinge region at residue position 121 of Pim-1. Other kinases also form a second conserved hydrogen bond between the N1 atom of adenine and the backbone NH of the third hinge residue (corresponding to residue 123 of PIM-1), this bond acceptor and donor in the hinge region serves as the kinase family structural signature [15]. Unlike other kinases, residue 123 in Pim-1 is Proline, thus restricting all possibilities of forming additional bonds for being the imino acid. Additional residue insertion causes the region

to bulge out from the ATP binding pocket. Structurally it was found that Pim proteins are not much different while considering mutant and wild type proteins. Moreover, much difference was not there in P123M mutant and similar kinase proteins experimentally. Crystallization of this protein with or without ATP analogue as a co-crystallizer has been a daunting task. Attempts to co-crystallize P123M mutant with four other small molecules revealed no conformational change in the mutant structures vis-a-vis the wild-type protein, suggesting that it is unlikely that a bound ATP molecule is able to induce a large conformational change required to bring the backbone NH of M123 within hydrogen bonding distance to ATP. Interestingly, the wild-type Pim-1 and the mutant enzyme display identity in the hinge region of the structure and proving the fact of the contributions of specific residues for the stability of the same conserve region. A further experiment showed that a deletion of residue E124 in combination with P123M caused the protein to lose kinase activity completely and to fail to crystallize despite extensive trials. The adverse effect caused by shortening the hinge suggests that the typical length of the hinge is important for Pim-1.

Molecular Modeling studies have emerged as an efficient tool for understanding various molecular, structural and functional aspects of small and large molecules which includes ligands as well as biological macromolecules such as proteins. Thus far ample applications and utilization of such cost effective and sophisticated techniques has been immensely insightful to understand the molecules. Many a times, computational analysis generated exceptional lead for further experiments.

Software associated methodologies altered the perspective towards biological data analysis tremendously. Growing reliance on such computational methodologies allowed us to perform an in-depth study on the mentioned protein to unveil the molecular interactions of the protein and the ligands and to understand the small molecular quantum chemical and other properties responsible to specific interactions. Detail of the study method followed is provided in the following section.

Methodology

A molecular modeling based approach was adopted for this study to understand the structure of the Pim-1 protein along with the binding efficiency of various ligand molecules considered for this study. The following section describes the methods stepwise.

Data set and molecular modeling

A data set of 55 Pim-1 kinase inhibitors have been chosen from the literature, inhibitory activities was used for the present 3D-QSAR (MFA and RSA) studies (Table 1) [20,24,25]. During the 3D QSAR analysis, log IC50 values were considered as the dependent variables for computation. Sketching of the ligand molecules along with energy minimization and stability testing was performed using molecule builder module of cerius2 software on silicon graphics workstation. Training and test set of the molecules was divided as per the standard exercise protocol. 43 compounds were part of the training and 12 compounds were part of the testing dataset and proper statistical validation of the obtained model [20]. During energy minimization, OFF (open force field) method was opted along with steepest descent algorithm considering convergence criterion of 0.001 kcal/mol for each molecule. Gasteiger method was implemented for overcoming the problem of partial atomic charges [24].

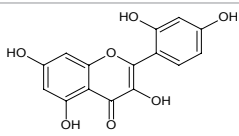
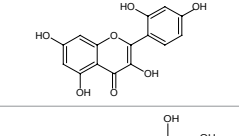
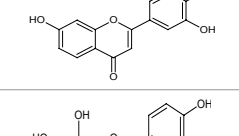
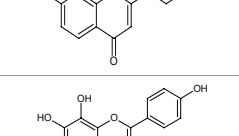
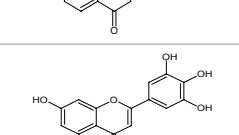
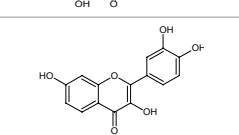
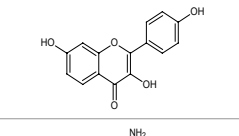
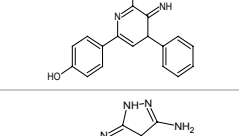
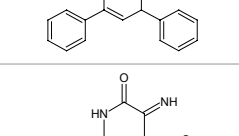
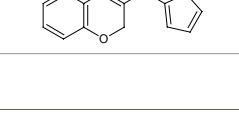
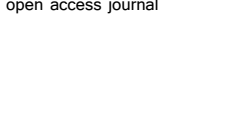
Generating conformations

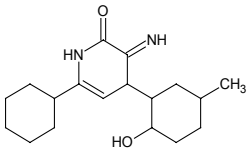
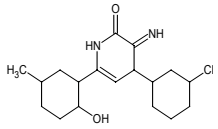
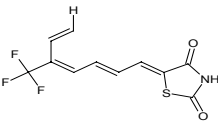
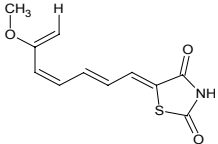
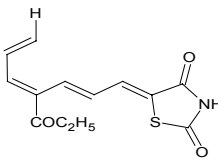
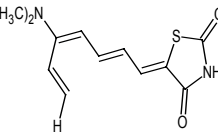
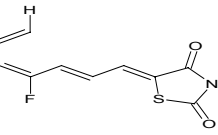
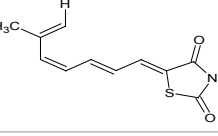
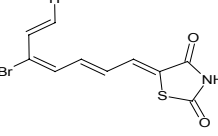
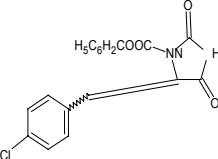
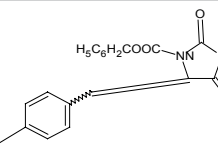
Several conformers are generated for each molecule applying the

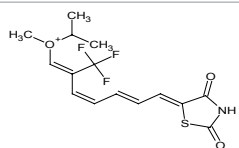
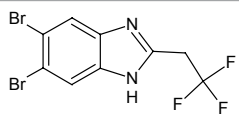
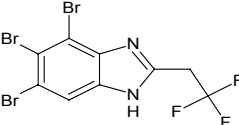
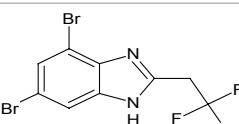
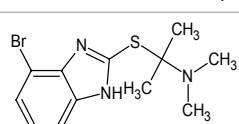
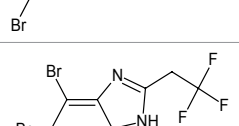
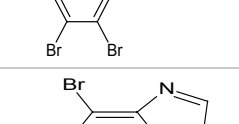
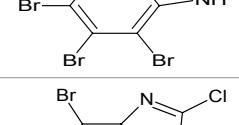
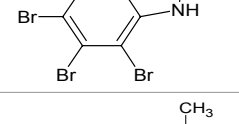
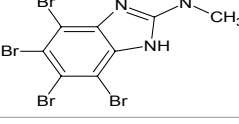
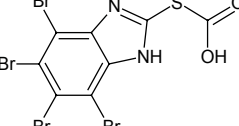
molecular sketching tools followed by a series of steps to attain the conformation with most favorable energy values. Molecular shape analysis (MSA) acts as a major data dimension for 3D QSAR analysis where structural conformational information for each molecule is considered. Multiple iterations are considered till the convergence while generating a QSAR equation satisfying the statistical significance. Obtained predicted values of the molecules during this study are provided in table 1. It was observed that the most active compound was 4-11 which was considered as the active conformer depending on the results (Table 1).

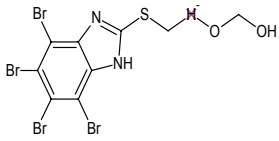
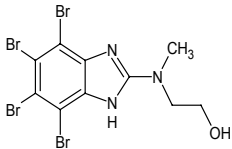
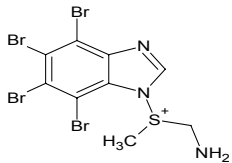
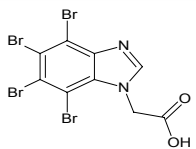
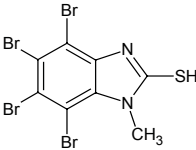
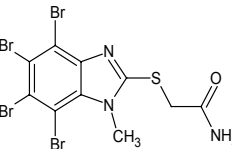
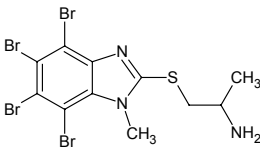
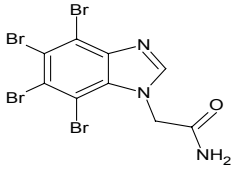
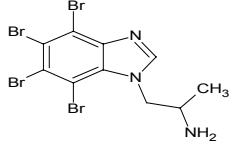
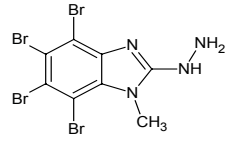
Alignment procedure

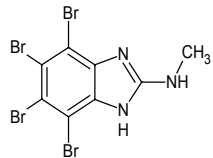
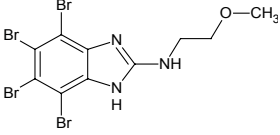
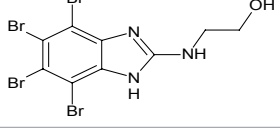
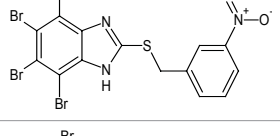
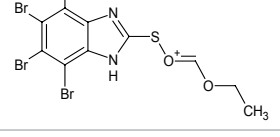
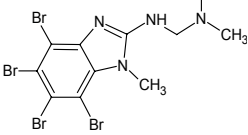
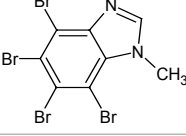
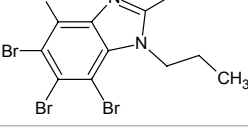
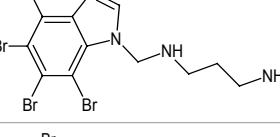
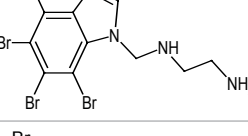
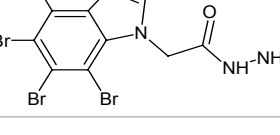
Cerius2 is having an excellent facility of aligning ligand molecules based on their shape reference during any QSAR analysis. Thus, same option with MCS (maximum common subgraph) and CSS (core substructure search) were utilized in this study. Considering the scaffold structure, all other molecules are aligned with its reference by super positioning the atoms in a pairwise manner (Figure 1) [21]. The implementation of the computation is done through a graph theory based approach considering the nodes and edges for each structure while aligning with the reference structure.

Structure no.	Structures	Exp IC50	MFA Predicted	Residual	RSA Predicted	Residual
1-2		3.4313	3.239	0.192	3.164	0.267
1-3		3.6551	3.852	-0.197	3.832	-0.177
1-5		3.8920	3.768	0.124	3.458	0.434
1-8		4.1461	4.353	-0.207	3.832	0.314
1-10		4.3424	4.109	0.234	3.832	0.510
1-14		2.8129	2.667	0.146	2.308	0.505
1-16		2.9294	2.926	0.004	3.558	-0.629
1-18		2.9912	3.238	-0.247	3.437	-0.446
2-1		3.6444	3.632	0.012	3.832	-0.188
2-2		3.6785	3.632	0.046	3.832	-0.153
2-4		3.680	3.632	0.048	3.852	-0.172

2-17		3.1731	3.632	-0.459	3.187	-0.014
2-19		3.5490	3.632	-0.083	3.907	-0.358
3-2		2.204	2.589	-0.388	2.832	-0.628
3-3		2.1139	2.229	-0.116	2.301	-0.187
3-5		2.7781	2.752	0.026	2.640	0.138
3-8		3.7781	3.351	0.427	3.413	0.365
3-9		2.2300	2.323	-0.096	2.202	0.028
3-11		2.5185	2.807	-0.289	2.269	0.250
3-15		3.7075	3.351	0.357	3.742	-0.034
3-18		4.4471	4.388	0.059	4.356	0.091
3-21		3.7781	3.632	0.146	3.716	0.062

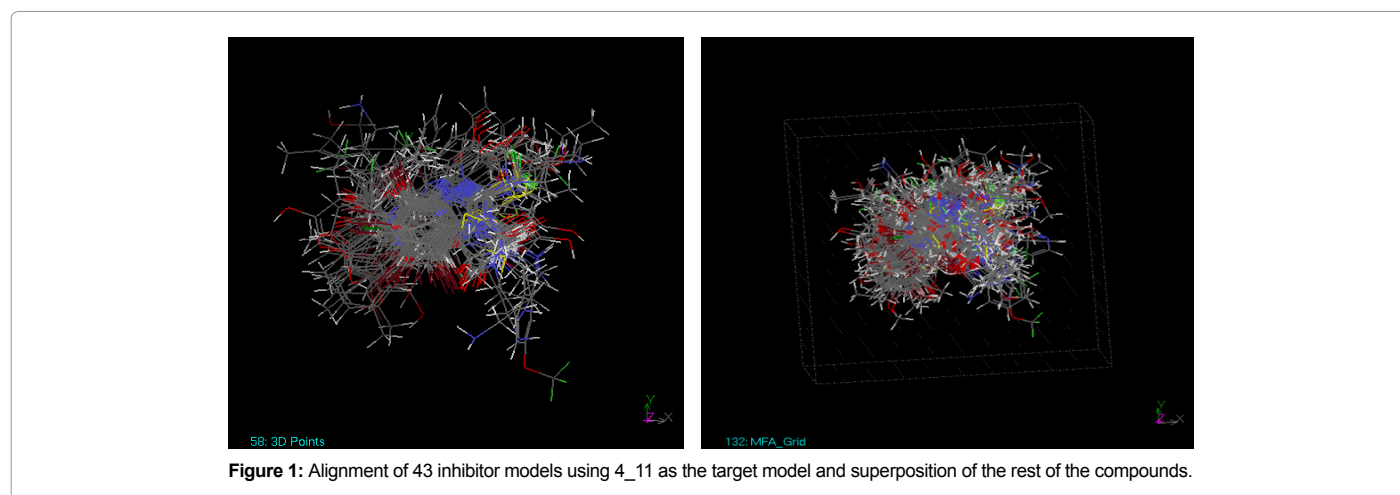
3-28		1.6020	2.237	0.210	2.638	-0.191
4-2		4.0791	4.131	-0.052	4.002	0.077
4-4		4.2068	4.128	0.078	4.172	0.035
4-5		3.9138	4.265	-0.351	4.153	-0.239
4-6		4.0253	4.061	-0.036	3.458	0.567
4-7		3.9956	4.045	-0.049	4.136	-0.140
4-11		4.910	4.787	0.122	4.711	0.199
4-15		3.7558	3.979	-0.223	3.831	-0.075
4-22		4.7489	5.018	-0.270	4.589	0.160
4-26		4.2944	4.522	-0.228	4.229	0.065
4-32		4.8733	4.828	0.045	5.028	-0.155

4-34		4.8369	4.742	0.095	4.290	0.547
4-39		4.6334	4.551	0.082	4.603	0.030
4-44		4.950	4.890	0.060	4.603	0.347
4-49		4.6117	4.780	-0.168	4.572	0.040
4-51		4.8202	4.553	0.267	4.524	0.296
4-52		4.6875	4.466	0.222	4.241	0.447
4-53		4.3729	4.185	0.188	4.478	-0.105
4-55		4.4533	4.640	0.222	4.229	0.224
4-56		4.4440	4.625	-0.181	4.229	0.215
4-59		3.9344	3.632	0.302	4.367	-0.433

4-17		3.5663	3.691	-0.134	3.918	-0.362
4-19		4.1818	4.391	-0.209	4.601	-0.419
4-23		4.9547	4.567	0.388	4.603	0.352
4-27		4.0211	3.990	0.031	4.426	-0.405
4-28		3.6232	3.538	0.085	3.940	-0.317
4-33		3.6334	3.783	-0.150	3.867	-0.234
4-35		4.6683	4.835	-0.155	4.599	0.069
4-37		3.7708	3.835	-0.064	4.218	-0.447
4-40		3.5910	3.335	0.256	4.229	-0.638
4-41		4.8573	4.670	0.187	4.229	0.628
4-57		4.7250	4.568	0.157	4.436	0.289

4-58		4.0128	4.066	-0.053	3.831	0.182
------	---	--------	-------	--------	-------	-------

Table 1: Training set and test set compounds with observed and predicted activities.



QSAR studies

Molecular field analysis (MFA): Further investigations during the QSAR study related to the Molecular field analysis (MFA) were carried out using Cerius2 [22]. A reference probe molecule is used for computing the similarities and differences of the aligned molecules present in a molecular field considered for a particular QSAR analysis. In this case, the probes used were electrostatic proton and other from steric methyl group. Continuous sampling of the fields was carried out by the algorithm with a grid space of 2 Å. Altogether 1750 grid points were generated along with consideration of energy cutoff of -30.0 kcal/mol and 30 kcal/mol for steric and electrostatic grid points respectively. The descriptors considered for this analysis were radius of gyration, molecular volume, polarizability, number of rotatable bonds, principle moments of inertia, dipole moment, number of hydrogen bond donors and acceptors, A log P, and molar refractivity. Only high variance containing descriptors were counted as independent variables in this study which was almost 10% of the total descriptors considered. Genetic partial least square (G/PLS) based regression was performed with 5000 generations and 100 population size and the number of optimum component was fixed at 5 for the present analysis. To obtain an unbiased score, the smoothing parameter, d, was set to 1.0. Further, leave-one-out based cross validation was conducted to rectify the biasness of the results. Normalization was conducted to receive equivalence in the variables and the variance was set to 1.0.

Receptor surface analysis (RSA): This particular analysis provide understanding about the essential information related to the receptor site as a three-dimensional surface along with information on the properties considered to map onto the surface model. The same set of aligned molecules was utilized to develop a receptor surface, using the Vander Waals field function. The contribution of each molecule in the generation of receptor surface is proportional to its biological activity. The most active compounds with the activity ranging from 1 nM to 5nM, were used to develop the Receptor Surface Model (RSM).

During this process, multiple chemical properties such as electrostatic potential (ELE), charge, hydrogen bond development tendency and hydrophobicity of every surface point were computed. Docking was conducted for the receptor with each molecule. The obtained results displayed the interaction energy and strain energy as an output of the docking calculations. Further, the interaction energies of each molecule with different probes situated along the grid points are considered as the outcome of the analysis.

Molecular docking: The program GOLD (Genetic Optimisation for Ligand Docking) was used for docking the inhibitors into the ATP site of the Pim-1 kinase protein [16]. GOLD is an extensively used docking program used for assessing ligand protein interaction. It applies genetic algorithm to analyze ligand conformational flexibility for a specific dock mode. The computation methodology maintains a rigorous monitoring towards fulfilling the basic requirement to remove the loosely bound water molecules upon the binding of the ligand molecules. A crystal structure of Pim-1 kinase (PDB code: 1XWS) was used for molecular docking studies.

Results and Discussion

Molecular field analysis (MFA)

In this study, molecular field analysis (MFA) was conducted using a series of hydroxyflavone, pyridone and thiazolidene-2,4-dione derivatives inhibitory activities (Table 1). The overall analysis contains a training set of 43 compounds and 12 compounds were used for validation of the obtained data as part of the test set. Table 1 represents the statistical information of the MFA analysis ($r^2=0.830$, $rcv^2=0.744$). The obtained results from the test and training set of MFA for the actual and predicted activities are displayed in this section where figure 2A provide the information on the actual versus predicted pIC50 values found for the training and the test set molecules.

The boot strapping BSR² value was 0.785. Variation in biological

activity owing to the structural variation of the ligands with relation to the electrostatic (H+) descriptors is provided in figure 2B. Favorable regions are indicated by the positive coefficient with electrostatic descriptor H+ whereas negative coefficient indicates electronegative. Location of the descriptors in the 3D grid is specified by the numbers associated. The equation generated by MFA model is given by the following Eq. (1).

$$1. \text{Activity} = 3.99869 + 0.049039 * \text{"H+/275"} - 0.023925 * \text{"H+/364"} - 0.100154 * \text{"H+/58"} + 0.02992 * \text{"H+/627"} + 0.03352 * \text{"H+/265"}$$

Presence of electrostatic descriptor (H+/364) at C7 position of 1-16 compounds in figure 2B of fisetin indicates that the importance of the electrostatic environment at this position. Certain facts were observed in compounds 1-2, 1-3, 1-5, 1-8, 1-10, 1-14 and 1-18. These inactive compounds were characterized in most cases by bulky (charged or uncharged) groups at the 3, 3', 4', or 7 positions; lack of at least two hydrogen bond donors on the A or C rings; presence of glycoside

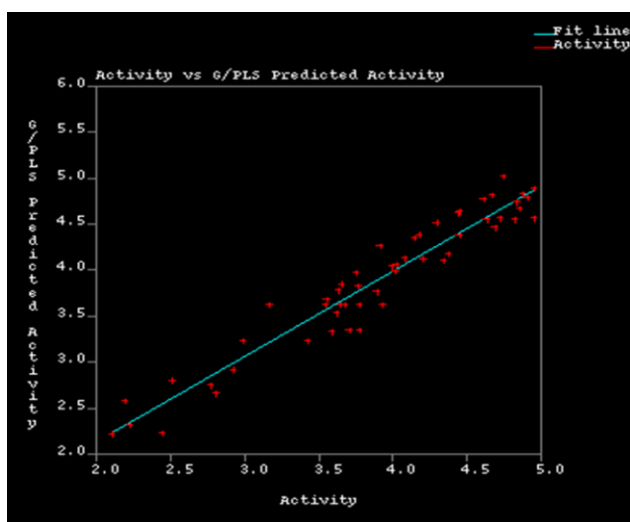


Figure 2A: Correlation graph between experimental and predicted activities of MFA.

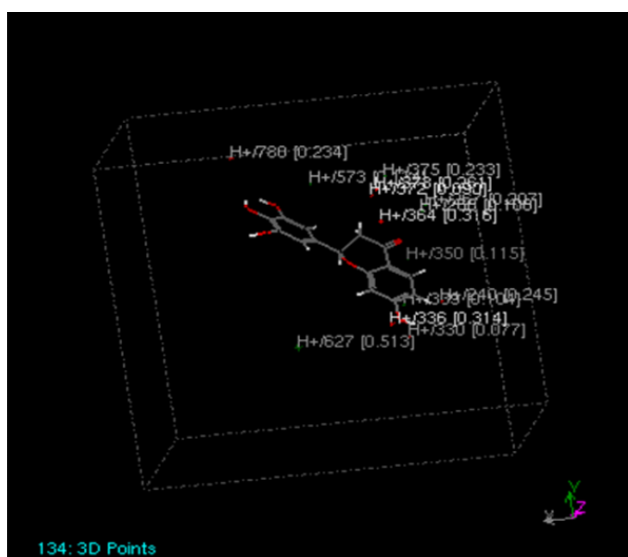


Figure 2B: MFA grid and grid points.

linkages; or failure of all rings to adopt a planar conformation. The most active compound in the chemical library was the flavonol quercetin (IC50=4.3424 nmol), a known inhibitor of kinases and many other enzymes. Furthermore, six of the eight compounds with reproducible activity at a range from 2.8 to 4.3 nmol were hydroxyl flavone. The four hydroxyl flavone with the highest inhibitory activity were characterized by the presence of five to six -OH groups distributed between the A and B rings. In comparison, the hydroxyl groups on the B ring seemed to be more critical for the activity of the compounds than those on the A ring, as compounds with an unsubstituted B ring showed greatly reduced activity.

A high rcv 2 alone is not enough for a QSAR model to be considered as robust and accurate. Therefore, generalization through prediction with the molecules not included in the training set was done using the standard equation: $r^2_{pred} = SD - PRESS / SD$, where SD refers to the sum of squared deviations between the biological activities of each molecule and the mean activity of the training set molecules and PRESS is the sum of squared deviations between the predicted and actual activity values for every molecule in the test set. Remaining 12 test set members were predicted correctly with an error less than 0.3. Possibly the conformational flexibility of methylene group between triazafluorenone ring and phenyl ring played a major role in this case. The predictive r^2 (rpred 2) value was found to be 7.912. Hence, the predictive ability of MFA model is high except for compound 1-16.

Receptor surface analysis (RSA)

A model based on receptor surface analysis using same training set molecules was developed, which were used in MFA studies. The cross-validated correlation coefficient of the generated model was (rcv2=0.646) and conventional $r^2=0.787$. The actual and predicted activities obtained from RSA model for the training and the test set molecules are shown in figure 3 respectively.

The van der waals (VDW) and electrostatic (ELE) descriptors in the QSAR equation of RSA (eq. 2) determines the regions related to the structural variation of different compounds in the training set, lead to increased or decreased activities with respect to the pseudo receptor surface generated.

The QSAR equation generated by RSA is given in following equation (2).

$$2. \text{Activity}_1 = 3.91556 + 52.5721 * \text{"ELE/4041"} + 150.452 * \text{"ELE/3791"} - 48.7618 * \text{"ELE/5181"}^2 + 29.0701 * \text{"VDW/2481"}^2 - 1139.12 * \text{"ELE/2931"} + 0.010522 >^2.$$

The equation consists of five receptor field descriptors. The positioning of these descriptors, indicated by a number along with the descriptors, on the model explains the nature of the substituents required. The presence of one positive coefficient steric descriptor (VDW/2481) and two positive coefficient electrostatic descriptors (ELE/4041, ELE/3791) at N4 position of amine group explains the need of a moderately bulky is required at this position.

Two electronic descriptors (ELE/4041, ELE/3791) present same position explains the need of a bulky and electron withdrawing substituent. Further, the steric descriptor (VDW/ 2481) with positive coefficient present near the ortho-position of N4 amine group, indicate that any steric group increase the activity. When the charge is mapped on the receptor surface model, it shows a negative contour (red color) near the ELE/5181 descriptor (Figure 4).

This indicates that an electronegative environment is essential at

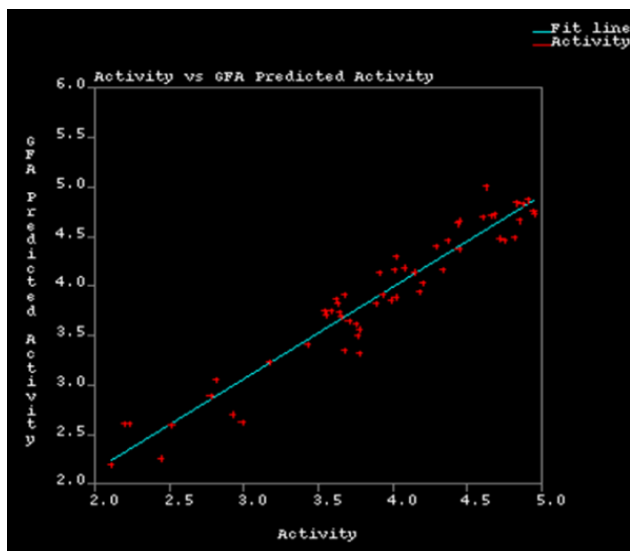


Figure 3: Output of the correlation between experimental and predicted activities of RSA.

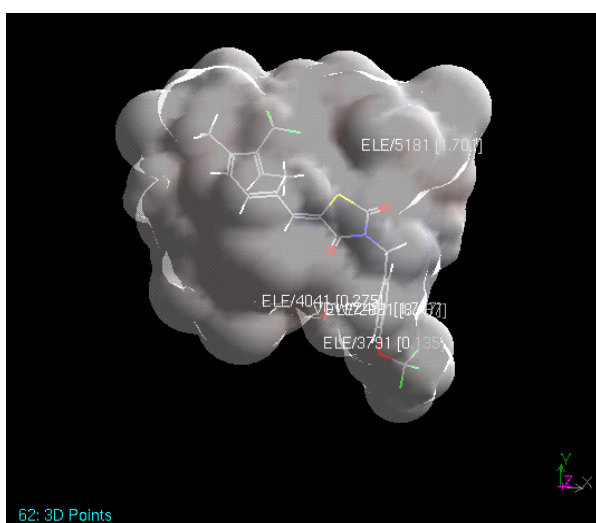


Figure 4A: Receptor surface model with charges mapped on to it. Positive regions are shown in blue and negative regions are shown in red. Compound 3-28 is placed within the generated receptor surface.

this position. A blue color contour is observed near to S in the ring indicating the importance of hydrophobic group is essential at these positions. Hydrogen bonding properties are mapped on the receptor surface as shown in figure 4C. The figure illustrates that only hydrogen bond acceptor property is observed in receptor surface model.

Cyan color shows hydrogen bond acceptor properties. The cyan color was seen in close proximity of the ELE/5181 descriptor region indicating that hydrogen bond acceptor groups are quite essential at these positions. As shown in figure 4B, brown color indicates the hydrophobic area, while white color indicates hydrophilic area.

The RSA model was further validated using the same test set molecules as in MFA. RSA predicted 100% of molecules correctly with an error less than 0.5. The predictive r2 (rpred 2) value was found to

be 6.631. Hence, the predictive ability of RSM model is also high. MFA had a lower value of rcv 2 of 0.823, while RSA had a higher rcv2 value 0.869. This rcv2 of MFA indicates good external consistency compared

Component	MFA	RSA
Cross-validated (r ²).	0.744	0.869
Conventional (r ²).	0.830	0.909
Dep SD	30.923	16.653
Bootstrap r ² .	0.785	0.910
Predictive r ² .	4.638	6.631
Dep mean	3.892	3.869

Table 2: Statistics obtained after MFA and RSA analysis of the 3D-QSAR models.

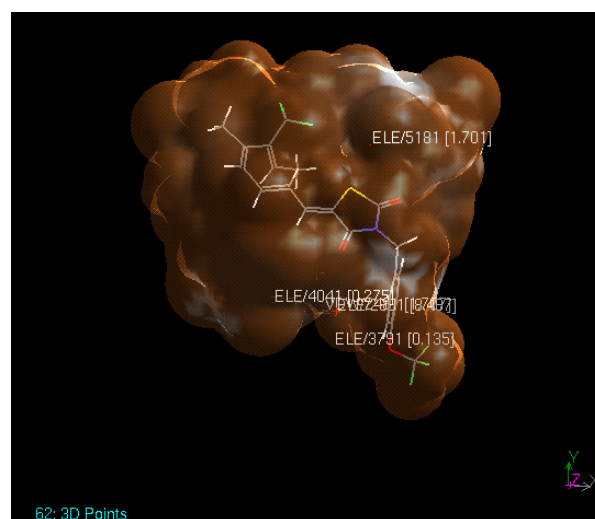


Figure 4B: Receptor surface model with hydrophobic regions mapped on it. Hydrophobic regions are shown in brown and hydrophilic regions are shown in white.

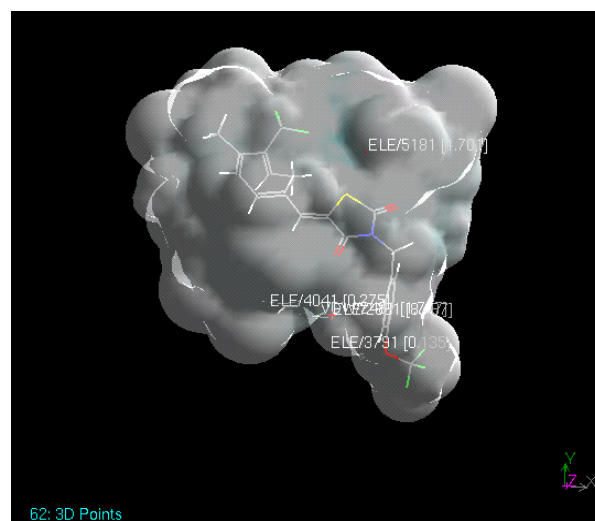


Figure 4C: Receptor surface model with hydrogen bonding property mapped on it. Hydrogen bond donor regions are shown in purple, while hydrogen bond acceptor regions are shown in cyan color.

to RSA, whereas in RSA, the residual value is 0.6.631 rpred 2 values, for MFA is 4.638. Overall both models have good predictive ability while MFA predicted well as compared to RSA.

Molecular docking results GOLD

GOLD fitness scores were compared with observed activity for all 55 molecules. All molecules shown in tables 1-4 were divided into three sets named low active (pIC50=2.230), moderately active (pIC50=2.929) and high active (pIC50=4.934) based on experimental pIC50 values. After performing docking, these three categories fell in the regions LEU44, PHE49, VAL52, LYS67, GLU89, GLU121, ARG122, PRO123, ILE185 of hinge region of the Pim-1 kinase protein. The observed predicted values in terms of GOLD fitness scores are shown in table 3. Compound (3-9) 5-arylidene-2,4-thiozolidinediones (Table 1) is experimentally low active but GOLD predicted as high active, which was built and docked

with crystal structure of Pim-1(PDB code:1XWS) using the suite of programs within material studio interface (Accelrys) as its structure is similar to compound (3-2)5-(3-trifluoromethylbenzene) thiazolidine-2,4-dione that better activity values observed via experiments and high predicted score [25]. The only structural difference is the presence of Florine group at R1 substitution instead of trifluoromethyl group. As

Fitness	S(hb_ext)	S(vdw_ext)	S(hb_int)	S(int)
36.05	1.09	26.49	0.00	-1.47
36.03	6.36	31.14	0.00	-13.15
48.52	10.00	31.58	0.00	-4.90

Note: hb_ext (protein-Ligand external hydrogen bond energy); vdw_ext (Protein-ligand van der Waal energy); hb_int (Protein-ligand internal hydrogen bond energy) were compared

Table 3: Fitness values of the best-ranked ligand docked using GOLD software.

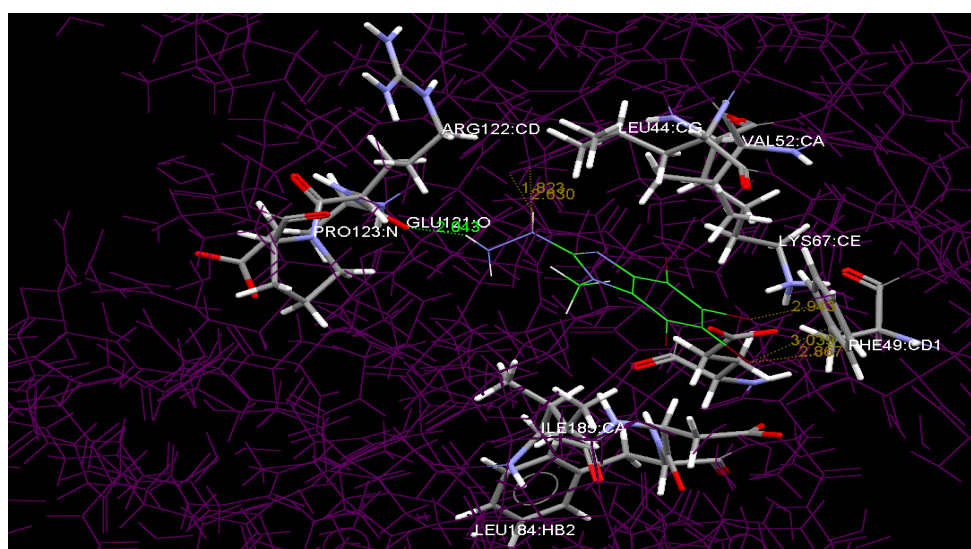


Figure 5A: Docking of the inhibitor in the hinge region of Pim-1 ATP region.

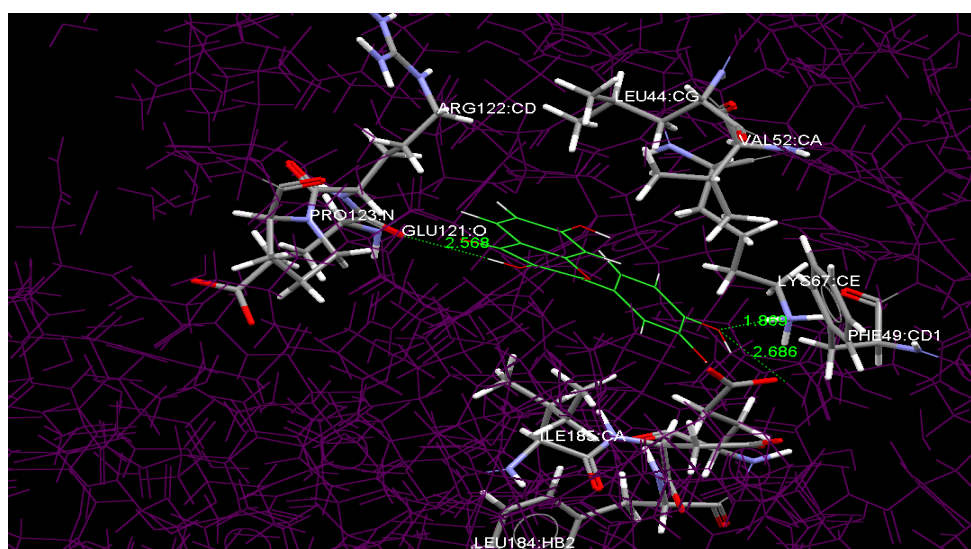


Figure 5B: Active site was visualized with the docked ligand.

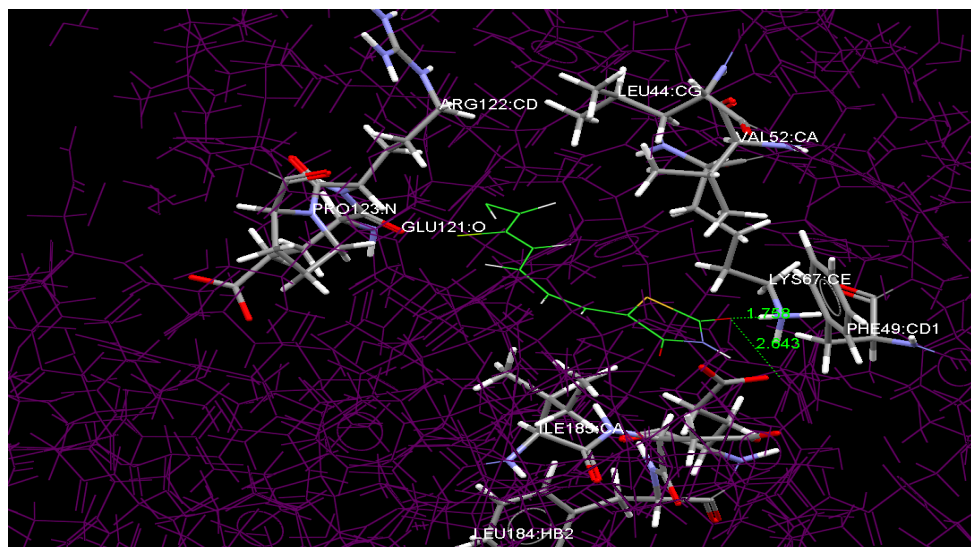


Figure 5C: Active site was visualized with the docked ligand..

the binding mode for 3-9 in which the thiazolidine NH group donates a H-bond to the carbonyl oxygen of GLU121 and these results suggest that the thiazolidine ring in particular is a good candidate for modification as according to the pharmacophore model (Table 1) this ring system only contributes a hydrogen bond to the hinge region while making few other non-bonded contacts. The carbonyl groups could be replaced with hydrophobic functionality in order to exploit contacts with PRO 123 and LEU44. Predicted fitness scores for high and low active compounds are shown in table 3. The hydrogen bond distances are 1.758 with LYS67, 2.643 with water. The hydrogen bonding interactions with the moderate active molecule (compound 1-16) and high active molecule (compound 4-59) were also observed (Figure 5). The high active molecule has shown hydrogen bond distance of 2.043 with GLU121 and few hydrophobic bonds distance of 1.823, 2.630, 2.943, 3.039, 2.867 nearer to PHE49. The moderate active molecule has shown hydrogen bond distance of 2.568 with GLU121, 1.809 with LYS67 and 2.686 with water. So, all the interactions are within the hinge region of the Pim-1. It was found that Van Der Waals interactions were also dominant at the active site. This can be supported by citing a comparison between the inactive compounds which has no groups attached to the 2-amino position of all the inhibitors and the active compound or others groups. In the active site region, these groups exhibit Van Der Waals interactions (Tables 4-6). The acquired fitness scores are represented in table 6. Finally, the binding pocket of the active site was visualized with the docked ligand in figure 5.

Conclusion

Human civilization has faced the impact of various diseases on and off throughout our existence. Multiple life threatening diseases, such as malaria [25-30], tuberculosis [23], HIV [31,32], other viral diseases [33], diabetes and associated diseases [34,35] affected our life again and again. Recent incidence of such impact has been recorded in the literature regularly. Various approaches have been adopted by the modern science to tackle such situation. Enormous experimental efforts are there to come out with viable solutions but experimental technologies require support from modern theoretical, computational and data analysis methodologies. Theoretical analysis has become

Mol No	Fitness	S(hb_ext)	S(vdw_ext)	S(hb_int)	S(int)
1	34.67	0.00	25.48	0.00	-0.37
2	34.73	0.00	25.66	0.00	-0.56
3	36.05	1.09	26.49	0.00	-1.47
4	35.57	0.00	27.86	0.00	-2.73
5	33.32	0.00	24.43	0.00	-0.28
Average Value	34.87	0.22	25.99	0.00	-1.08

Table 4: Van Der Waals interactions.

Mol No	Fitness	S(hb_ext)	S(vdw_ext)	S(hb_int)	S(int)
1	32.53	1.01	30.60	0.00	-10.56
2	36.03	6.36	31.14	0.00	-13.15
3	35.67	6.05	30.98	0.00	-12.98
4	35.83	6.36	31.04	0.00	-13.21
Average Value	35.02	4.95	30.94	0.00	-12.47

Table 5: Van Der Waals interactions.

Mol No	Fitness	S(hb_ext)	S(vdw_ext)	S(hb_int)	S(int)
1	48.52	10.00	31.58	0.00	-4.90
2	47.98	9.76	1.47	0.00	-5.06
3	48.47	10.00	31.93	0.00	-5.42
Average Value	48.32	9.92	31.66	0.00	-5.13

Table 6: Acquired fitness scores.

the most important support to experimental validations and able to reduce the time frame of an experiment via almost accurate predictive approaches. In-depth computational analysis along with molecular modeling studies have become part of the medicinal chemistry and bimolecular analysis research and providing novel information on the disease associated targets.

In this analysis, 3D-QSAR and molecular docking studies were

carried out to explore the binding mechanism of hydroxyflavanone, thiazolidene 2,4-dione, pyridone derivatives against Pim-1, and to construct highly predictive 3D-QSAR models for designing new moloney murine leukemia virus inhibitors for the treatment of leukemia cells and a number of other myeloid and lymphoid tumor and prostate tumor line diseases. The presence of the hydroxyl groups on the B ring seemed to be more critical for the activity of the compounds than those on the A ring, as compounds with an un-substituted B ring showed greatly reduced activity. Further, the steric descriptor (VDW/ 2481) with positive coefficient present near the ortho-position of N4 amine group, indicate that any steric group increases the activity. The presence of electrostatic and steric groups strongly favored both in RSA and MFA models. For molecular docking, 55 molecules were considered which were docked in Pim-1 ATP binding site and possible ranking was done in terms of overall binding affinity. Our prediction showed that fitness scores correlated well with experimental activity available for the molecules. Thus, this specific study provided new guidelines for novel inhibitor design to accelerate the drug discovery process.

References

- Holder S, Lilly M, Brownd ML (2007) Comparative molecular field analysis of flavonoid inhibitors of the PIM-1 kinase. *Bioorg Med Chem* 15: 6463-6473
- Tao ZF, Hasvold LA, Levenson JD, Han EK, Guan R, et al. (2009) Discovery of 3H-Benzo[4,5]thieno[3,2-d]pyrimidin-4-ones as potent, highly selective, and orally bioavailable inhibitors of the human protooncogene proviral insertion site in moloney murine leukemia virus (PIM) kinases. *J Med Chem* 52: 6621-6636.
- Akue-Gedu R, Rossignol E, Azzaro S, Knapp S, Filippakopoulos P, et al. (2009) Synthesis, kinase inhibitory potencies, and in vitro anti proliferative evaluation of new pim kinase inhibitors. *J Med Chem* 52: 6369-6381.
- Keane NA, Reidy M, Natoni A, Raab MS, O'dwyer M (2015) Targeting the Pim kinases in multiple myeloma. *Blood Cancer J* 5: e325.
- Pagano MA, Bain J, Kazmierczuk Z, Sarno S, Ruzzene M, et al. (2008) The selectivity of inhibitors of protein kinase CK2. *J Biochem* 415: 353-365.
- Holder S, Zemskova M, Zhang C, Tabrizizad M, Bremer R, et al. (2007) Characterization of a potent and selective small-molecule inhibitor of the PIM-1 kinase. *Mol Cancer Ther* 6: 163-172.
- Cheney WI, Yan S, Appleby T, Walker H, Vo T, et al. (2007) Identification and structure-activity relationships of substituted pyridones as inhibitors of Pim-1 kinase. *Bioorg Med Chem Lett* 17: 1679-1683.
- Brizzi MF, Dentelli P, Rosso A, Yarden Y, Pegoraro L (1999) STAT protein recruitment and activation in c-Kit deletion mutants. *J Biol Chem* 274: 16965-16972.
- Olla S, Manetti F, Crespan E, Maga G, Angelucci A, et al. (2009) Indolylpyrrolone as a new scaffold for Pim-1 inhibitors. *Bioorg Med Chem Lett* 19: 1512-1516.
- Grey R, Pierce AC, Bemis GW, Jacobs MD, Moody CM, et al. (2009) Structure-based design of 3-aryl-6-amino-triazolo[4,3-b]pyridazine inhibitors of Pim-1 kinase. *Bioorg Med Chem Lett* 19: 3019-3022.
- Katayama K, Yamaguchi M, Noguchi K, Sugimoto Y (2014) Protein phosphatase complex PP5/PPP2R3C dephosphorylates P-glycoprotein/ABCB1 and down-regulates the expression and function. *Cancer letters* 345: 124-131.
- Xia Z, Knaak C, Ma J, Beharry ZM, McInnes C, et al. (2009) Synthesis and evaluation of novel inhibitors of Pim-1 and Pim-2 protein kinases. *J Med Chem* 52: 74-86.
- Natarajan K, Xie Y, Burcu M, Linn DE, Qiu Y, et al. (2013) Pim-1 kinase phosphorylates and stabilizes 130 kDa FLT3 and promotes aberrant STAT5 signaling in acute myeloid leukemia with FLT3 internal tandem duplication. *PLoS One* 8: e74653.
- Solomon KA, Sundararajan S, Abirami V (2009) QSAR studies on N-aryl derivative activity towards alzheimer's disease. *Molecules* 14: 1448-1455.
- Cozza G, Girardi C, Ranchio A, Lolli G, Sarno S, et al. (2014) Cell-permeable dual inhibitors of protein kinases CK2 and PIM-1: structural features and pharmacological potential. *Cell Mol Life Sci* 71: 3173-3185.
- Zheng GZ, Bhatia P, Daanen J, Kolsa T, Patel M, et al. (2005) Structure-activity relationship of triazafluorenone derivatives as potent and selective mGluR1 antagonists. *J Med Chem* 17: 7374-7388.
- Bharatham N, Bharatham K, Lee KW (2006) Quantitative structure-activity relationships and molecular docking studies of P56 LCK inhibitors. *Bulletin of Korean chemical society* 27: 266-272.
- Desiraju GR, Gopalakrishnan B, Jetti RKR, Raveendra D, Sarma JARP (2000) Three-Dimensional quantitative structural activity relationship (3D-QSAR) studies of some 1,5-Diarylpyrazoles: Analogue based design of selective cyclooxygenase-2 inhibitors. *Molecules* 5: 945-955.
- Kumar A, Mandiyan V, Suzuki Y, Rice CZJ, Tsai J, et al. (2005) Crystal structures of proto-oncogene kinase Pim-1: A target of aberrant somatic hyper mutations in diffuse large cell lymphoma. *J Mol Biol* 348: 183-193.
- Pierce AC, Jacobs M, Stuver-Moody C (2008) Docking study yields four novel inhibitors of the protooncogene Pim-1 kinase. *J Med Chem* 51: 1972-1975.
- Bachmann M, Tarik M (2005) The serine/threonine kinase Pim-1. *Int J Biochem Cell Biol* 37: 726-730.
- Rogers D, Hopfinger AJ (1994) Application of genetic function approximation to quantitative structure-activity relationships and quantitative structure-property relationships. *J Chem Inf Comput* 34: 854-866.
- Gasteiger J, Marsili M (1980) Iterative partial equalization of orbital electronegativity-A rapid access to atomic charges. *Tetrahedron* 36: 3219-3228.
- Sekhar YN, Ravikumar M, Nayana MRS, Mallena SC (2008) 3D-QSAR studies of triazafluorenone inhibitors of metabotropic glutamate receptor subtype 1. *Eur J Med Chem* 43.5: 1025-1034.
- Zheng GZ, Bhatia P, Kolsa T, Patel M, El Kouhen OF, et al. (2006) Correlation between brain/plasma ratios and efficacy in neuropathic pain models of selective metabotropic glutamate receptor 1 antagonists. *Bioorg Med Chem Lett* 16: 4936-4940.
- Banerjee AK, Arora N, Murty U (2012) Analyzing a potential drug target N-Myristoyltransferase of Plasmodium falciparum through in silico approaches. *J Glob Infect Dis* 4: 43-54.
- Banerjee AK, Arora N, Murty US (2009) Structural model of the Plasmodium falciparum thioredoxin reductase: a novel target for antimalarial drugs. *J Vector Borne Dis* 46: 171-183.
- Arora N, Chari UM, Banerjee AK, Murty U (2007) A computational approach to explore Plasmodium falciparum 3D7 chorismate synthase. *Int J Genomics Proteomics* 3: 3-28.
- Arora N, Banerjee AK, Murty US (2010) Homology model of 2C-methyl-erythritol 2, 4-cyclodiphosphate (MECP) synthase of Plasmodium falciparum 3D7. *Electron J Biol* 6: 52-57.
- Banerjee AK, Arora N, Murty US (2012) Aspartate carbamoyltransferase of Plasmodium falciparum as a potential drug target for designing anti-malarial chemotherapeutic agents. *Medicinal Chemistry Research* 21: 2480-2493.
- Shinde SP, Banerjee AK, Arora N, Murty US, Sripathi VR, et al. (2015) Computational approach for elucidating interactions of cross-species miRNAs and their targets in Flaviviruses. *J Vector Borne Dis* 52: 11-22.
- Arora N, Banerjee AK (2012) New targets, new hope: novel drug targets for curbing malaria. *Mini Rev Med Chem* 12: 210-226.
- Arora N, Banerjee AK (2012) Targeting tuberculosis: a glimpse of promising drug targets. *Mini Rev Med Chem* 12: 187-201.
- Saxena KS, Gupta A, Bhagyashree K, Saxena R, Banerjee AK, et al. (2012) Targeting strategies for human immunodeficiency virus: a combinatorial approach. *Mini Rev Med Chem* 12: 236-254.
- Banerjee AK, Murty US (2007) Extracting the significant descriptors by 2D QSAR and docking efficiency of NRTI drugs: a molecular modeling approach. *Internet J Genomics Proteomics*.